# Local Preserving Class Separation Framework to Identify Gestational Diabetes Mellitus Mother Using Ultrasound Fetal Cardiac Image

**ANJAN GUDIGAR[1], JYOTHI SAMANTH[2], U RAGHAVENDRA[1*], CHINMAY DHARMIK[1], AKHILA VASUDEVA[3], PADMAKUMAR R[4], RU-SAN TAN[5,6], EDWARD J CIACCIO[7], FILIPPO MOLINARI[8], U RAJENDRA ACHARYA[9,10,11]**

[1]Department of Instrumentation and Control Engineering, Manipal Institute of Technology, Manipal Academy of Higher Education, Manipal 576104, India.
[2]Department of Cardiovascular Technology, Manipal College of Health Professions , Manipal Academy of Higher Education, Manipal 576104, India.
[3]Department of Obstetrics and Gynecology, Kasturba Medical College, Manipal Academy of Higher Education, Manipal 576104, India.
[4]Department of Cardiology, Kasturba Medical College, Manipal Academy of Higher Education, Manipal 576104, India.
[5]National Heart Centre Singapore, Singapore
[6]Duke-NUS Medical School, Singapore
[7]Department of Medicine Division of Cardiology, Columbia University Medical Center, USA.
[8]Department of Electronics and Telecommunications, Politecnico di Torino, Italy
[9]Department of Electronics and Computer Engineering, Ngee Ann Polytechnic, Clementi 599489, Singapore.
[10]Department of Biomedical Engineering, School of Science and Technology, SUSS University, Clementi 599491, Singapore.
[11]International Research Organization for Advanced Science and Technology (IROAST) Kumamoto University, Kumamoto, Japan.

Corresponding author: U Raghavendra (e-mail: raghavendra.u@manipal.edu)

**ABSTRACT** In the presence of gestational diabetes mellitus (GDM), the fetus is exposed to a hyperinsulinemia environment. This environment can cause a wide range of metabolic and fetal cardiac structural alterations. Fetal myocardial hypertrophy predominantly affecting the interventricular septum possess a morphology of disarray similar to hypertrophic cardiomyopathy, and may be present in some GDM neonates after birth. Myocardial thickness may increase in GDM fetuses independent of glycemic control status and fetal weight. Fetal echocardiography performed on fetuses with GDM helps in assessing cardiac structure and function, and to diagnose myocardial hypertrophy. There are few studies in the literature which have established evidence for morphologic variation associated with cardiac hypertrophy among fetuses of GDM mothers. In this study, fetal ultrasound images of normal, pregestational diabetes mellitus (preGDM) and GDM mothers were used to develop a computer aided diagnostic (CAD) tool. We proposed a new method called local preserving class separation (LPCS) framework to preserve the geometrical configuration of normal and preGDM/GDM subjects. The generated shearlet based texture features under LPCS framework showed promising results compared with deep learning algorithms. The proposed method achieved a maximum accuracy of 98.15% using support vector machine (SVM) classifier. Hence, this paradigm can be helpful to physicians in detecting fetal myocardial hypertrophy in preGDM/GDM mothers.

**INDEX TERMS** Fetal myocardial hypertrophy, Gestational diabetes mellitus, Local preserving class separation, Computer-aided diagnosis, Ultrasound images

## I. INTRODUCTION

DIABETES in pregnancy is one of the common risk factors for adverse perinatal outcomes, with a prevalence of 7% to 11% in India and up to 17% in South India [1], [2]. Neonates born to diabetic mothers — either gestational diabetes mellitus (GDM) or pregestational diabetes mellitus (preGDM), that is, with diabetes only during or pre-existing before pregnancy, respectively— are at risk of cardiovascular disease due to structural cardiac defects or impaired myocardial function. Fetal circulation is fundamentally different from neonatal circulation. There are structural and functional adaptations that take place in response to a hypoxemic intrauterine environment [3], [4]. Fetal cardiac changes that are demonstrated on imaging, are known to have influence

**IEEE** *Access*

on neonatal outcome [5]. In GDM, this developmental abnormality ranges widely from structural heart disease to subclinical myocardial dysfunction [6]–[8]. The hyperinsulinemic state interferes with fetal metabolism, resulting in increased expression and affinity of insulin receptors, which leads to proliferation and hypertrophy of cardiac myocytes. Cardiac hypertrophy in these fetuses exhibits myocardial derangement similar to hypertrophic cardiomyopathy [9]. This disarray in myofiber alignment alters the diastolic function of the heart. GDM fetuses sometimes exhibit cardiac diastolic dysfunction even in the absence of cardiac hypertrophy [10]. GDM manifests comprehensive adverse effects ranging from subclinical cardiac involvement to neonatal complications requiring medical attention. Subtle cardiac dysfunction has been confirmed by speckle tracking echocardiography. Most recently, use of four-dimensional (4D) ultrasonography along with two-dimensional (2D) fetal cardiac imaging showed promising results in the detection of cardiac malfunction early in pregnancy [11]–[13]. Therefore, screening fetal cardiac structure and function among GDM and preGDM mothers could be helpful to identify subtle pathology early in gestation [14]. Maintaining adequate glycemic control in these groups may help prevent fetal complications related to GDM. Computer-Aided Detection/Diagnosis (CAD) uses a rule-based support system for patient diagnosis. At present, it is utilized in numerous applications in day-to-day clinical practice. For instance, in detecting breast malignancies, skeletal abnormalities, and pathology in brain and vascular tissues. The need for CAD in our study is evident because of the poor prognosis of the disease if left untreated. GDM or preGDM may lead to fetal death, which can be averted if diagnosed early and strict glucose control measures are implemented. The CAD in this study is based on ultrasound (US) imaging. Many recent studies have proposed accurate CAD models using US images [15]–[23]. Physicians can typically distinguish or identify the disease by manual interpretation of the images, but the process is intensive, induces fatigability, and is prone to bias and human error. Fetal myocardial hypertrophy (FMH) ranges from subtle to overt myocardial hypertrophy, and the clinical course is heterogeneous. Few works have been published in the literature on this topic. There have been a few works recently that examined the thickness of the interventricular septum (IVS), which separates the left and right ventricles, in FMH. Carolina et al. [24] evaluated the prevalence of FMH in the fetuses of pregnant women with GDM, and they found that 54% of 63 fetuses tested positive for FMH on fetal echocardiography. Mohammed et al. [25] employed five-dimensional (5D) fetal echocardiography for the diagnosis of prenatal fetal hypertrophic cardiomyopathy on three separate groups: healthy members, controlled diabetic mothers, and uncontrolled diabetic mothers. They obtained a maximum mean IVS thickness of 0.57± 0.08 cm for a group of 37 uncontrolled diabetic mothers. They also suggested that the infants of diabetic mothers could reverse FMH, provided these neonates are given special care and constant monitoring. A similar study is reported in [26].

The fetal state is evaluated using fetal heart rate (FHR) with the help of continuous wavelet transform and convolutional neural network (CNN) [27]. They have achieved an accuracy of 98.34%. In [28], the authors have used recurrence plot and CNN to achieve an accuracy of 98.69% using FHR signals. We believe that the CAD model presented herein is the first to be developed for the detection of FMH in preGDM/GDM mothers. The major contributions of the paper are:

•The shearlet based texture features are generated to characterize the normal and preGDM/GDM US images.

•The discriminative capability of the locality sensitive discriminant analysis (LSDA) is enhanced under local preserving class separation framework.

•To the best of our knowledge, this is the first work to identify the fetal cardiac structure of gestational diabetes mellitus mother automatically using US images.

The remainder of the paper is structured as follows. The description of dataset and details of the proposed methodology is delineated in Section II. The experimental results and the comparative study are presented in Section III. The results are analyzed and discussed in Section IV. The paper ends with a conclusion and future scope, which is provided in section V.

## II. MATERIALS AND METHODS

### A. DATA ACQUISITION

A case control study was performed in a tertiary referral hospital from March 2017 to March 2019. In this study, pregnant women with preGDM and GDM having a gestational age between 32 and 37 weeks were included. Non-diabetic healthy pregnant women at similar gestational age served as controls. Women with preeclampsia, pre-existing hypertension treated with antihypertensive drugs, renal disease, liver disease, hematologic diseases, maternal cardiac disease, evidence of fetal congenital anomaly of any organ including heart, intrauterine growth retardation, chromosomal abnormalities, and twin pregnancy were excluded from the study. Institutional Ethics Committee approval was obtained. Informed written consent was obtained from all participants. PreGDM mothers had known diabetes before the pregnancy. GDM was diagnosed using the International Association of Diabetes in Pregnancy Study Group criteria for oral glucose tolerance test (blood glucose cutoffs of 93/183/152 mg% at baseline/1 hour/2 hours following 75 gm oral glucose) between gestational age 24-28 weeks. All participants underwent fetal echocardiographic examination. Trained obstetrician imaged the cardiac chambers and stored at end diastolic frame of 4-chamber view. Likewise, a trained sonographer measured the parameters. In each subject, a standard lateral 4-chamber view was obtained. In total, we enrolled 74 normal subjects (at least two images from each subject, total: 221 images) and 71 preGDM/GDM subjects (at least two images from each subject, total: 212 images) in this study. Figure 1 shows sample normal and abnormal US subjects.
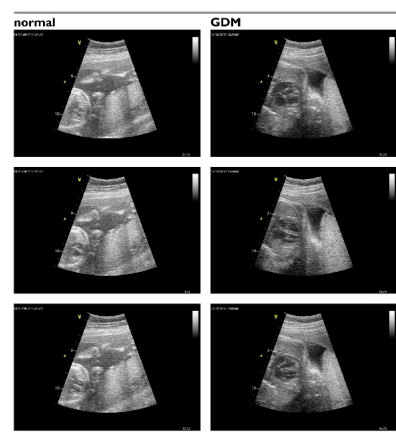
**FIGURE 1.** Ultrasound images of fetal hearts from normal and diabetic mother.



**FIGURE 2.** Architecture of proposed model.

## B. PROPOSED METHOD

Figure 2 highlights the active modules of the proposed approach. It consists of three modules namely: i) feature extraction, ii) subspace learning, and iii) classification. In the first stage shearlet based texture features are extracted to characterize US images. In the second stage the data were reduced by using local preserving class separation method. Herein, local manifold structure of each class and discrimination among the classes are embedded efficiently, while representing the data in lower dimensional space. Further in the last stage, support vector machine (SVM) was used to classify the ranked features with different kernels. The detailed description of each stage is explained in the subsequent section.

### 1) Shearlet based texture features

Initially, every image is preprocessed, where mask is generated using morphological close operation to extract region of interest [29]. The application of mask helps to remove the labels, color map indication etc. Further the resultant image is rescaled to a predefined size i.e., $256 \times 256$ pixels for generality purpose. In the next step, shearlet transform is used generate the shearlet coefficients. Shearlets are very efficient tools for directional representation compared to wavelets [30]. They are used in many applications for better representation of the images [31], [32]. They consist of functions with parabolic scaling, shearing operators and translation operators that can be used to change resolution, orientation and position, respectively. Sometimes, a more precise shearlet system is referred to as cone-adapted, as it is adapting a cone-like structure in frequency domain. To have flexible shearlets, a parameter is introduced in the scaling matrix for measuring anisotropy [33]. The generating functions are associated with the conic and low frequency regions [34]. On the other hand, for data restoration and feature extraction techniques, shearlets with optimal sparse representation perform better. In this work, scale of 2 is used to get twenty coefficients.
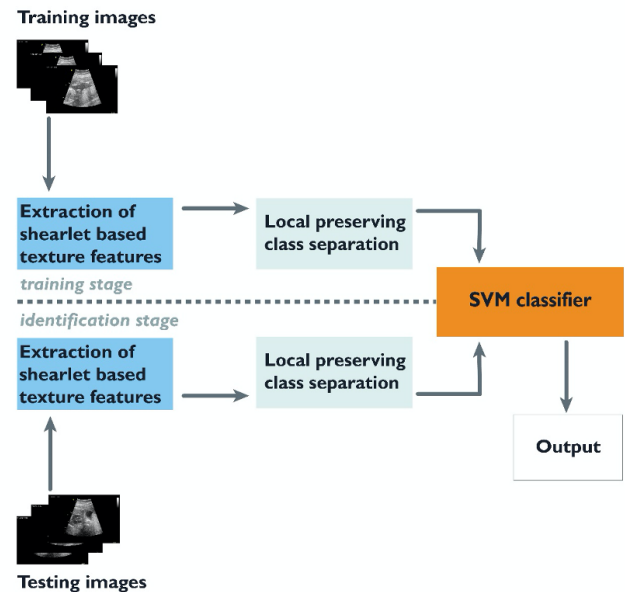
Generally, textures convey significant information of an image that pertains to the structural arrangement and relationship between neighboring pixels [35]. For pattern recognition, various texture features can be generated using gray-level co-occurrence matrix (GLCM). It is the function of nearest pixels' distance with angular relationship. In this study, GLCM is calculated for angles 0, 45, 90, and 135 degrees. For every GLCM, the features information correlation measures 1 and 2, energy, correlation, contrast, homogeneity, difference entropy and difference variance, sum variance, sum entropy and sum average as defined in [35] and cluster shade, maximum probability, autocorrelation, entropy, and dissimilarity as defined in [36] are calculated. Finally, the average value of all the features that are computed from each GLCM is computed to describe the US image. Usually, coarse texture and fine texture have long and short gray level runs, respectively [37]. For a given image, textures were extracted from the run-length matrix (RLM). The features formulated in [38], [39] were extracted and the combination of gray level and run length were used to obtain various statistical measures [40]. As a result, 11 features pertaining to RLM were extracted. Furthermore, variance, kurtosis, and skewness were also computed for every shearlet coefficient. Hence, thirty features were calculated for each shearlet coefficient. A total of 600 shearlet based texture features are generated for each US image. The complete process of feature extraction is shown in Figure 3.
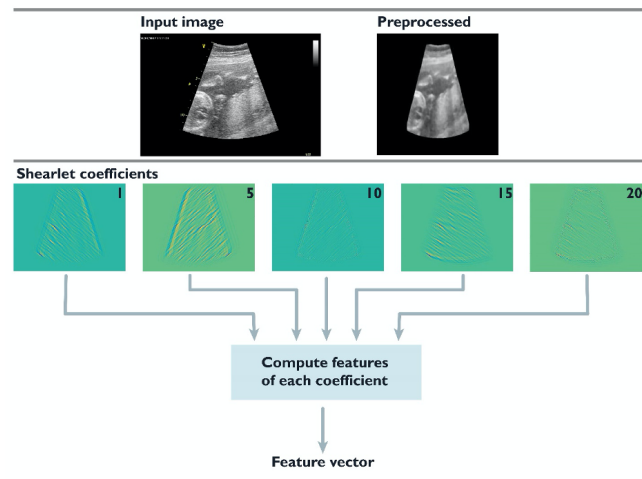
**FIGURE 3.** Generation of feature vector using shearlet coefficients.

### 2) Local preserving class separability

Generally, the local structure of the data points becomes more important than its global structure when training samples are insufficient [41], [42]. Linear discriminant analysis (LDA) is widely used in many applications to maximize the separation between data points from various classes [43]. In practice, subspace learning is performed by mapping whereby data points with different labels are isolated from each other whereas data points with the same label points are aggregated close to each other. When data points exhibit non-linearity, then preserving the local structure of the data points is the primary requirement for efficient training. Hence in this paper, local preserving class separability (LPCS) algorithm was introduced to enhance the discrimination power of LSDA method. The proposed LPCS consists of two steps, which are described as follows,

Initially, weight matrix is computed to describe the local structure of the data points. Consider a data points $x_1, x_2, ... ..., x_r$ in $\mathbb{R}^q$, where r is the data points. The directed edge is placed between the nodes if data points are k-nearest neighbors, i.e., if there is an edge between nodes i and j, then it can be denoted as $i \sim j$. The weight matrix $w_{ij}$ has the value of the edge weight if there is existence of edge between i and j, otherwise it is zero [41]. Further, the projection using neighborhood preserving is performed to preserve the required local distribution of the data points. The obtained new space $\mathbb{R}^n$, where n«q, is used for further class separation.

In the second step, mapping is performed using the between-class and within-class graphs ($g_d^{'}$ and $g_s^{'}$, respectively). Consider a map on new space as $y^{'} = (y_1^{'}, y_2^{'}, \cdots, y_r^{'})^T$, and the following objective functions are used for better mapping. [43]:

$$min \sum_{i'j'} \left( y_i^{'} - y_j^{'} \right)^2 w_{s,ij}^{'} \qquad (1)$$

$$max \sum_{i'j'} \left( y_i^{'} - y_j^{'} \right)^2 w_{d,ij}^{'} \qquad (2)$$

where $w_{s,ij}^{'}$ is defined as 1 if neighbors share the same label, $w_{d,ij}^{'}$ is defined as 1 if neighbors have different labels on new space $\mathbb{R}^n$. The above equations are solved by using $y^{'} = Z^T x^{'}$, where Z is the projection matrix. Hence, the dimension reduction technique using LPCS method completely preserves both the local geometrical structure as well as discrimination of the data. Finally, LPCS is used to reduce the dimension of the shearlet based texture features efficiently.

### 3) Classification

Further, generated features with greater differences between the means and standard deviations(SD) were selected, and subjected to classification in order to determine the accuracy. Typically, extracted features contain some insignificant and excess information, which may debase the arrangement process. To make an effective arrangement model, a Student's t-test based highlight choice calculation was utilized [44] and features were ranked based on p-values. The ranked features were subjected to classifiers with different kernels. In the present study, we used the SVM classifier [45]–[47]. In many cases, linear functions cannot separate the data. Mapping input data into a different space is a solution. Here, kernel functions were employed as the dot product had been used on the training data. Therefore, the decision function using kernel functions could be included with SVM, and is denoted by K( ,). For a given K( ,), test sample h is given by:

$$f(h) = sign\left( \sum_{i=1}^{N} \lambda_i l_i K(v_i, h) + b \right) \qquad (3)$$

where N is the number of support vectors (SVs), $\lambda_i$ is Lagrange multipliers, $l_i$ is the labels, $v_i$ are the SVs, and b indicates the bias term. In our study, we used two basic kernel functions: polynomial (with 1, 2, and 3 order) and radial basis function (RBF). For RBF kernel scaling factor is varied from 1 to 5 to achieve maximum result. To assess the system performance, classification accuracy, sensitivity, specificity, and positive predictive values (PPV) were calculated. A *ten-fold* cross validation strategy was used to validate the technique. In *ten-fold* cross validation, the dataset is first split into *ten* equal parts with *nine* parts being used for training to test on the remaining *one* part; and the process is repeated ten times, which means that each part participates in testing once.

### III. RESULT

The complete algorithm was implemented using MATLAB environment on an Intel core i5 system with 4GB RAM. The generated shearlet features for every US image were reduced to thirty LPCS features. The LPCS features are ranked in descending order using its t-value as shown in Table 1. Then these ranked LPCS features were classified using SVM classifier with one-against-all strategy. Table 2 shows the performance of SVM classifier with different kernels. It

4

**IEEE** Access·

**TABLE 1.** Statistical details (Mean, SD, p-value and t-value) of LPCS features.

| Features | Normal | | preGDM/GDM | | p-Value | t-Value |
|---|---|---|---|---|---|---|
| | Mean | SD | Mean | SD | | |
| LPCS 10 | -2.6456 | 0.0818 | -2.6876 | 0.0728 | 3.15E-08 | 5.635757 |
| LPCS 6 | -2.5853 | 0.1041 | -2.6278 | 0.0870 | 5.68E-06 | 4.595326 |
| LPCS 7 | 8.2466 | 0.0852 | 8.2082 | 0.0934 | 1.01E-05 | 4.467531 |
| LPCS 3 | 13.0484 | 0.0976 | 13.0919 | 0.1208 | 4.42E-05 | 4.126719 |
| LPCS 1 | -1.4851 | 0.6124 | -1.2454 | 0.6363 | 7.65E-05 | 3.993743 |
| LPCS 5 | 6.0943 | 0.1153 | 6.0530 | 0.1035 | 0.000105 | 3.915837 |
| LPCS 4 | 1.9324 | 0.1126 | 1.9702 | 0.0916 | 0.000151 | 3.822911 |
| LPCS 2 | 10.7941 | 0.2165 | 10.7294 | 0.1987 | 0.001317 | 3.233401 |
| LPCS 8 | 5.3723 | 0.0845 | 5.3480 | 0.0795 | 0.002211 | 3.078843 |
| LPCS 9 | 4.3397 | 0.0853 | 4.3170 | 0.0702 | 0.00274 | 3.012875 |

**TABLE 2.** Performance of proposed system.

| #Fea | tp | tn | fp | fn | accuracy(%) | PPV(%) | sensitivity(%) | specificity(%) |
|---|---|---|---|---|---|---|---|---|
| SVM+POLY1 | | | | | | | | |
| 15 | 173 | 181 | 40 | 39 | 81.75 | 81.22 | 81.60 | 81.90 |
| SVM+POLY2 | | | | | | | | |
| 30 | 197 | 196 | 25 | 15 | 90.76 | 88.73 | 92.92 | 88.68 |
| SVM+POLY3 | | | | | | | | |
| 28 | 210 | 215 | 6 | 2 | 98.15 | 97.22 | 99.05 | 97.28 |
| SVM+RBF | | | | | | | | |
| 15 | 204 | 213 | 8 | 8 | 96.30 | 96.22 | 96.22 | 96.38 |
| #Fea, number of features; fp, false positive; fn, false negative; tp, true positive; tn, true negative | | | | | | | | |

is observed that proposed system achieved 98.15% accuracy, 97.22% PPV, 99.05% sensitivity, and 97.28% specificity using twenty-eight features. The performance obtained for individual features is shown in Figure 4. It is noted that SVM+POLY3 achieved 16.4%, 7.39%, and 1.85% higher accuracy compared to POLY1, POLY2, and RBF kernels, respectively. To assess the performance of the proposed system, comparative study was carried out, which is described in the subsequent section.
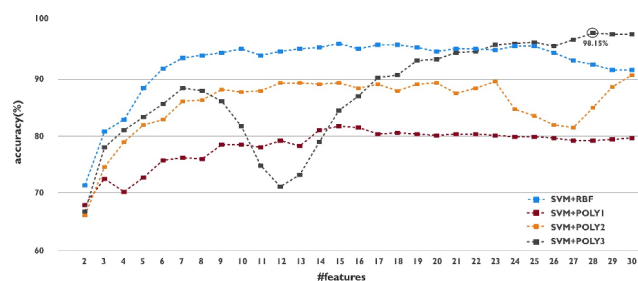


**FIGURE 4.** Performance of different classifiers using individual features one at a time. #features, number of features

## A. COMPARATIVE STUDY

The efficiency of the proposed LPCS was verified by comparing various data reduction techniques. In the present study, principal component analysis (PCA) [48], independent component analysis (ICA) [49], neighborhood preserving embedding (NPE) [41], and LSDA [43] were used. Figure 5 shows the performance in terms of accuracy of the various data reduction techniques with different numbers of features used. It is observed that the peak performance of the proposed LPCS method achieved improvements of 38.8%, 41.34%, and 15.01% compared with the peak performances of PCA,

ICA, and NPE techniques, respectively. The proposed LPCS increased the accuracy of LSDA by approximately 2%. It is also noted that sensitivity of LSDA increased by 4.72%, which is an important requirement for medical image analysis.
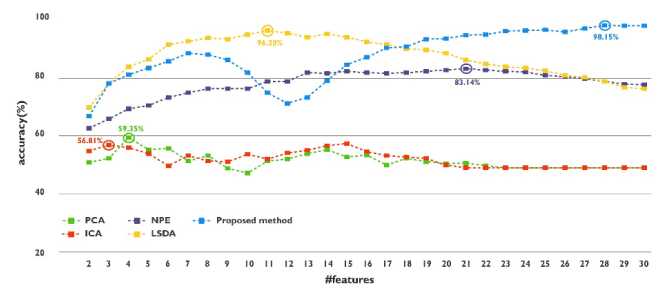


**FIGURE 5.** Performance of various data reduction techniques.

**TABLE 3.** Table 3: Structure of various used ConvNet.

| ConvNet-1 | ConvNet-2 | ConvNet-3 |
|---|---|---|
| Convolution1 (8 3×3 convolutions) | Convolution1(8 3×3 convolutions) | Convolution1(8 3×3 convolutions) |
| ReLU1 | ReLU1 | ReLU1 |
| Max Pooling1 (3×3 max pooling with stride [2 2]) | Max Pooling1 (3×3 max pooling with stride [2 2]) | Max Pooling1 (3×3 max pooling with stride [2 2]) |
| Convolution2(16 3×3 convolutions) | Convolution2 (16 3×3 convolutions ) | Convolution2(16 3×3 convolutions ) |
| ReLU2 | ReLU2 | ReLU2 |
| Max Pooling2 (3×3 max pooling with stride [2 2]) | Max Pooling2 (3×3 max pooling with stride [2 2]) | Max Pooling2 (3×3 max pooling with stride [2 2]) |
| | Convolution3 (32 3×3 convolutions) | Convolution3(32 3×3 convolutions) |
| | ReLU3 | ReLU3 |
| | Max Pooling3 (3×3 max pooling with stride [2 2]) | Max Pooling3 (3×3 max pooling with stride [2 2]) |
| | | Convolution4(64 3×3 convolutions) |
| | | ReLU4 |
| | | Max Pooling4 (3×3 max pooling with stride [2 2]) |

Nowadays, deep learning algorithms are increasingly bring applied to many applications, such as face recognition, traffic sign recognition system, medical image analysis, etc. using large datasets. Herein, we assessed how the proposed technique compare against various deep learning techniques. Six different deep network structures were considered for feature extraction: AlexNet [50] (please refer to https://in.mathworks.com/help/deeplearning/ref/alexnet.html), ResNet50 [51] (please refer to https://in.mathworks.com/help/deeplearning/ref/resnet50.html), GoogleNet [52](please refer to https://in.mathworks.com/help/deeplearning/ref/googlenet.html),

**IEEE** *Access*

**TABLE 4.** Comparison with state-of-the-art deep learning techniques

| Method | accuracy(%) | sensitivity(%) | specificity(%) |
|--------|-------------|----------------|----------------|
| AlexNet | 95.99 | 96.12 | 95.97 |
| ResNet50 | 78.83 | 79.37 | 79.08 |
| GoogleNet | 75.79 | 77.39 | 75.01 |
| ConvNet -1 | 60.46 | 62.11 | 61.12 |
| ConvNet -2 | 70.46 | 74.71 | 68.88 |
| ConvNet -3 | 81.39 | 82.34 | 81.53 |
| Proposed | 98.15 | 99.05 | 97.28 |



**FIGURE 6.** Plot of feature distribution a) original feature space and b) LPCS feature space.

and three convolutional neural network (ConvNet) models (i.e., ConvNet-1, ConvNet-2, and ConvNet-3)(please refert to https://in.mathworks.com/help/deeplearning/ug/create-simple-deep-learning-network-for-classification.html). In the present study AlexNet, ResNet50, and GoogleNet is used with a depth of 8, 50, and 22 respectively (please refer to https://www.mathworks.com/help/deeplearning/ug/pretrained-convolutional-neural-networks.html). Herein we have used pretrained networks for classification. Since the data set is comparatively small it is difficult to fine tune the parameters. Hence a feature extraction is done by using the layer activations of pretrained network as features. The structure of used ConvNet-1, ConvNet-2, and ConvNet-3 is shown in Table 3. For classification, SVM classifier was used, with scale and box constraint is equal to 1. Initially, US images were used and all images were preprocessed to remove artefacts and extract the regions of interest. Further, they were rescaled to predefined sizes: 64 × 64 for ConvNet and 224 × 224 for other networks. During classification, data was divided into ten equal parts, and 90% and 10% were used for training and testing, respectively, for 10 times until all parts had been tested. The networks were trained with a stochastic gradient decent with the momentum trainer using learning rate of 0.1, 0.01, and 0.001 with epochs of 10, 20, 30, 40, and 50, and is used by keeping two iterations per epoch with data shuffled per epoch. It is observed that the network achieved maximum result for learning rate of 0.01 and epoch of 30. It is also noted that all ConvNet models have achieved maximum results for image size of 64 × 64 when compared to 32 × 32 and 128 × 128. Ten passes of each network were obtained, and accuracy, sensitivity and specificity were calculated. From Table 4, it can be seen that among the 6 Networks AlexNet was relatively more consistent and accurate. On the other end, ConvNet-1 was unreliable and inconsistent. It is noted that ResNet50 and GoogleNet were quite consistent with similar output ranges. It is observed from Table 4 that our proposed model showed promising results compared with deep learning techniques.

## IV. DISCUSSION

Myocardial hypertrophy in the fetus and its associated complications require further study. There are different causes of FMH, including inheritable genetic diseases. Here, we have focused on acquired FMH associated with diabetes in pregnancy. Myocardial hypertrophy is identified commonly in fetuses of mothers with diabetes, and is characterized by thickening of the IVS or more subtle abnormalities. In a diabetic mother, high levels of insulin cause hyperplasia and hypertrophy of the fetal heart, resulting in FMH. We have developed a CAD model that can differentiate normal fetuses from affected fetuses. Few other methods exist of this particular capability in the literature. A prenatal IVS thickness greater than 4.5 mm has been reported to be an indication that the fetus has FMH [53]. In the current study, the mean values of myocardial thickness measured at IVS, left ventricular wall, and right ventricle among preGDM/GDM cases were higher than that of non-diabetic controls. The mean values in preGDM/GDM with adequate glycemic control were also higher than those in non-diabetic controls (data not shown). We did not report the prevalence of FMH in our study subjects as there is no standard threshold for defining FMH in South Indian, where the study had been carried out.

We applied shearlet transform, enhanced edges and curve-like structures in the images, to improve the quality of the 2D US images. It minimized redundant features and enhanced only significant information in the images. Further, texture variations in these coefficients were captured using various texture features. To differentiate the structure of normal versus preGDM/GDM images, we developed the LPCS method. The resultant feature distribution in a lower dimensional space is shown in Figure 6. It characterizes local structure and amplifies discrimination among classes, which boost its superiority compare with other data reduction techniques as shown in Figure 5.

Figure 6 shows the strength of the proposed method in discriminating the two classes, which enabled the classifier to generate the hyperplane easily. Although the normal and preGDM/GDM classes exhibited similar structures, the proposed LPCS separated the features in an efficient way. To our knowledge, this is the first work carried out to develop a CAD tool to categorize fetal cardiac structure using US in GDM mothers. The advantages of the proposed method are:

•The proposed features can efficiently characterize the heart structure.

•The LPCS method is generalizable and can be applied to the images of various modalities.

•The performance evaluated using ten-fold cross validation

is robust.

•It is computationally efficient and can be deployed in rural hospitals for screening.

## A. FUTURE SCOPE

This is the first CAD model that has been developed for the detection of fetal abnormalities associated with preGDM/GDM. In the future, the method can be combined with ConvNet, which may yield a higher probability for identifying disease. One limitation of our work is that we have only analyzed 433 digital images belonging to two classes. We are planning to include more images to further test the algorithm. In addition, a future direction for the CAD system will be to develop an Internet of Things (IoT) based model that can analyze the input images from a remote place, and send the results of analysis to both doctors and patients. This type of advanced screening tool can assist both doctors in their routine screening and follow-up of diabetic mothers. Figure 7 shows the future IoT based CAD model, where cloud based image analysis is proposed. The antenatal results need to be scrutinized to ensure that fetuses with FMH are identified immediately. The test can also be performed after birth for neonatal monitoring.
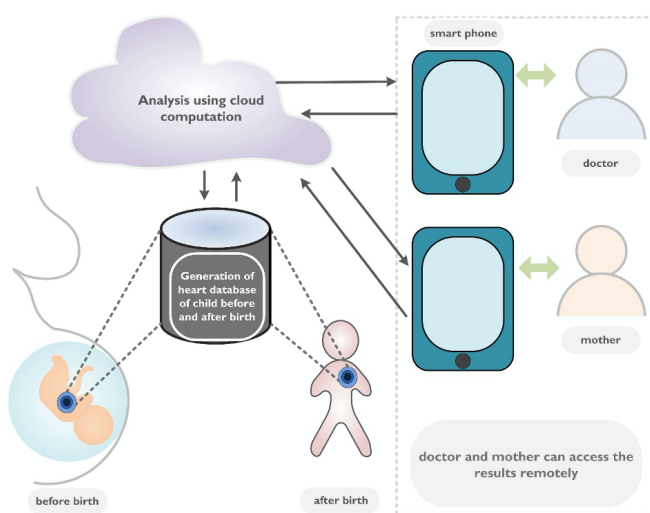


**FIGURE 7.** IoT based CAD tool for the detection of FMH.

## V. CONCLUSION

We studied fetal US images obtained from 74 normal subjects and 71 diabetic mothers. The shearlet based texture features showed remarkable performance under the LPCS framework using only twenty-eight features. The results were promising and should lead to more studies on the automatic detection of FMH with greater number of subjects, including studies involving ante- as well as post-natal US examinations. This will help clinicians better understand the longitudinal disease progression in FMH.

**IEEE** *Access*

## References

[1] Rajesh Rajput, Yogesh Yadav, Smiti Nanda and Meena Rajput, "Prevalence of gestational diabetes mellitus & associated risk factors at a tertiary care hospital in Haryana," *Indian Journal of Medical Research*, vol. 137, no. 4, pp.728-733, May 2013.

[2] Seshiah V., Balaji V., Balaji M. S., Paneerselvam A *et al.*, "Prevalence of gestational diabetes mellitus in South India (Tamil Nadu)–a community based study",*The Journal of the Association of Physicians of India* vol. 56, pp. 329-33, May 2008.

[3] Tan, Cheryl Mei Jun and Adam James Lewandowski,"The Transitional Heart: From Early Embryonic and Fetal Development to Neonatal Life."*Fetal diagnosis and therapy*, vol. 47, pp. 373-386, Sept. 2019.

[4] Youssef, Lina; Miranda, Jezid; Paules, Cristina; García Otero Laura*et al.,* "Fetal cardiac remodeling and dysfunction is associated with both preeclampsia and fetal growth restriction." *American Journal of Obstetrics & Gynecology*, vol. 222, no. 1,pp. 79.e1 - 79.e9, July 2019.

[5] Nilkant S. Phad, Koert de Waal, Carl Holder and Christopher Oldmeadow "Dilated hypertrophy: a distinct pattern of cardiac remodeling in preterm infants." *Pediatric Research* vol. 87,no. 1, pp. 146-152, Sept. 2019.

[6] Turan S., Turan O.M., Miller J., Harman C.*et al.* "Decreased fetal cardiac performance in the first trimester correlates with hyperglycemia in pregestational maternal diabetes." *Ultrasound Obstet Gynecol* vol. 38,no. 3, pp. 325-31, April 2011.

[7] Jyotsna A. Gandhi, Xiao Yang Zhang and Jack E. Maidman, "Fetal cardiac hypertrophy and cardiac function in diabetic pregnancies", *American Journal of Obstetrics and Gynecology*, vol 173, no. 4, pp. 1132-1136, Oct. 1995.

[8] Jose Garcia-Flores, Mercedes Jañez, Maria Cruz Gonzalez, Nuria Martinez *et al.* "Fetal myocardial morphological and functional changes associated with well-controlled gestational diabetes." *European journal of obstetrics, gynecology, and reproductive biology* vol. 154, no. 1, pp. 24-26, Jan 2011.

[9] Mehta A, and K Hussain. "Transient hyperinsulinism associated with macrosomia, hypertrophic obstructive cardiomyopathy, hepatomegaly, and nephromegaly." *Archives of disease in childhood* vol. 88 ,no. 9, pp. 882-884, Sept. 2003)

[10] Muhammad Mohsin, Saleem Sadqani, Kamran Younus, Zahra Hoodbhoy *et al.* "Evaluation of cardiac function in fetuses of mothers with gestational diabetes." *Cardiology in the young* vol. 29, no. 10, pp. 1264-1267, Oct. 2019.

[11] Huidong Li, Fanghua Peng, Chao Wu, Dexuan Kong *et al.* "Diagnostic value of four-dimensional ultrasonography with STIC combined with two-dimensional ultrasonography for fetal cardiac malformation and chromosomal abnormalities in early pregnancy." *Experimental and Therapeutic Medicine*,vol. 19, no. 2, pp. 1161-1166, Dec. 2019.

[12] Bo Wang, Jianning Li and Juan Yin "Diagnostic value of echocardiography in fetal cardiac malformation and clinical classification." *Experimental and Therapeutic Medicine* vol. 18, no. 3, pp. 1595-1600, July 2019.

[13] Noortje H. M. van Oostrum, S. Guid Oei and Judith O. E. H. van Laar "Normal fetal cardiac deformation values in pregnancy; a prospective cohort study protocol." *BMC Pregnancy Childbirth* vol.19, pp. 524, Dec 2019.

[14] Joshua Copel, "Fetal cardiac abnormalities: Screening, evaluation, and pregnancy management" *UpToDate* , Mar 2019, https://www.uptodate.com/contents/ fetal-cardiac-abnormalities-screening-evaluation-and-pregnancy-management

[15] Raghavendra U., Acharya U. R., Gudigar A., Shetty R. *et al.* "Automated screening of congestive heart failure using variational mode decomposition and texture features extracted from ultrasound images." *Neural Computing and Applications.* Vol. 28, No. 10, pp. 2869-2878, Oct 2017.

[16] Anjan Gudigar,U Raghavendra, Tom Devasia,Krishnananda Nayak *et al.*"Global weighted LBP based entropy features for the assessment of pulmonary hypertension", *Pattern Recognition Letters*, vol. 125, pp. 35-41, Jul. 2019. https://doi.org/10.1016/j.patrec.2019.03.027

[17] U Rajendra Acharya, U Raghavendra, Joel E W Koh, Kristen M Meiburger *et al.* "Automated detection and classification of liver fibrosis stages using contourlet transform and nonlinear features", *Computer methods and programs in biomedicine*, Vol. 166, pp. 91-98, Nov. 2018.

[18] U. Rajendra Acharya, Ayesha Akter, Pradeep Chowriappa, Sumeet Dua *et al.* "Use of Nonlinear Features for Automated Characterization of Suspicious Ovarian Tumors Using Ultrasound Images in Fuzzy Forest Framework", *International Journal of Fuzzy Systems, Springer*, Vol. 20, No. 4, pp. 1385-1402, Feb. 2018.

[19] U Raghavendra, Anjan Gudigar, M Maithri, Arkadiusz Gertych *et al.* "Optimized multi-level elongated quinary patterns for the assessment of thyroid nodules in ultrasound images", *Computers in biology and medicine*, Vol. 95, pp. 55-62, Apr. 2018.

[20] Filippo Molinari, U. Raghavendra, Anjan Gudigar, Kristen M. Meiburger *et al.* "An Efficient Data Mining Framework for the Characterization of Symptomatic and Asymptomatic Carotid Plaque using Bidimensional Empirical Mode Decomposition Technique", *Medical and Biomedical Engineering & Computing*, Springer, Vol. 56, No. 9, pp. 1579–1593, Feb. 2018.

[21] Raghavendra U., Fujita H., Gudigar A., Shetty R. *et al.* " Automated technique for coronary artery disease characterization and classification using DD-DTDWT in ultrasound images", *Biomedical Signal Processing and Control*, Vol. 40, Pp. 324-334, Feb. 2017.

[22] U R Acharya, O Faust, S V Sree, F Molinari *et al.* "Cost-effective and non-invasive automated benign and malignant thyroid lesion classification in 3D contrast-enhanced ultrasound using combination of wavelets and textures: a class of ThyroScan™ algorithms," *Technology in cancer research & treatment*, vol. 10,no. 4, pp. 371-80, Aug. 2011.

[23] Garcia-Canadilla P, Sanchez-Martinez S, Crispi F and Bijnens B, "Machine Learning in Fetal Cardiology: What to Expect." *Fetal diagnosis and therapy* vol. 47, no. 5, pp. 363-372, May 2020.

[24] Carolina Rossi Palmieri, Mona Adalgisa Simões, Jean Carl Silva, Anelise Darabas dos Santos *et al.* "Prevalence of Hypertrophic Cardiomyopathy in Fetuses of Mothers with Gestational Diabetes before Initiating Treatment." *Rev. Bras. Ginecol. Obstet.*, vol. 39, no. 1, pp. 9-13, Jan. 2017. [online].

[25] Mohammad AbdElhameed M. NasrAdDeen, Mohammed Salah Elsokkary, Mohamed Esmat Abbass Shawky and Heba Ramadan Elsayed Abdel Fattah "Diagnosis of Fetal Hypertrophic Cardiomyopathy in Diabetic Mothers Using 5D Fetal Echocardiography." *The Egyptian Journal of Hospital Medicine*, vol. 72, no. 7, pp. 4932-4937, Jul. 2018.

[26] Soares C, Olívia A, Lourenço C, Nogueira R *et al.*" A case of fetal hypertrophic cardiomyopathy in second trimester",in *15th World Congress in Fetal Medicine.*, Mallorca, Spain 2016.

[27] Zhidong Zhao, Yanjun Deng, Yang Zhang, Yefei Zhang *et al.* "DeepFHR: intelligent prediction of fetal Acidemia using fetal heart rate signals based on convolutional neural network."*BMC Medical Informatics and Decision Making*,vol. 19 , pp. 286, Dec. 2019. https://doi.org/10.1186/ s12911-019-1007-5

[28] Zhidong Zhao1, Yang Zhang, Zafer Comert and Yanjun Deng, "Computer-Aided Diagnosis System of Fetal Hypoxia Incorporating Recurrence Plot With Convolutional Neural Network." *Frontiers in physiology* vol. 10, pp. 255, Mar. 2019, doi:10.3389/fphys.2019.00255

[29] J. Serra and P. Soille (Eds.),"Mathematical Morphology and Its Applications to Image Processing", *proceedings of the 2nd international symposium on mathematical morphology (ISMM'94)*, Barcelona, May 1993.

[30] Kutyniok Gitta, Lim Wang-Q and Reisenhofer Rafael. "ShearLab 3D: Faithful Digital Shearlet Transforms Based on Compactly Supported Shearlets." *ACM Transactions on Mathematical Software*,vol. 42, no. 1, pp. 5, Feb. 2016.

[31] U Rajendra Acharya, Hamido Fujita, Vidya K Sudarshan, Shu Lih Oh *et al.* "Automated characterization of coronary artery disease, myocardial infarction, and congestive heart failure using contourlet and shearlet transforms of electrocardiogram signal",*Knowledge-Based Systems*, vol. 132, pp. 156-166, 2017.

[32] Anjan Gudigar, U. Raghavendra, Tan Ru San, Edward J. Ciaccio *et al.* "Application of multiresolution analysis for automated detection of brain abnormality using MR images: A comparative study", *Future Generation Computer Systems*, vol.90, pp. 359-367, Jan 2019.

[33] Genzel Martin and Kutyniok Gitta, "Asymptotic Analysis of Inpainting via Universal Shearlet Systems." *SIAM Journal on Imaging Sciences.*, vol. 7, no. 4, pp. 2301- 2339, Jan. 2014.

[34] Kutyniok G., Labate D. "Introduction to Shearlets. In: Kutyniok G., Labate D. (eds) Shearlets." *Applied and Numerical Harmonic Analysis.* Birkhäuser, Boston, 2012.

[35] R. M. Haralick, K. Shanmugam and I. Dinstein, "Textural Features for Image Classification," *IEEE Transactions on Systems, Man, and Cybernetics*, vol. SMC-3, no. 6, pp. 610-621, Nov. 1973, doi: 10.1109/TSMC.1973.4309314.

[36] L. -. Soh and C. Tsatsoulis, "Texture analysis of SAR sea ice imagery using gray level co-occurrence matrices," *IEEE Transactions on Geoscience and Remote Sensing*, vol. 37, no. 2, pp. 780-795, March 1999, doi: 10.1109/36.752194.

[37] Xiaoou Tang, "Texture information in run-length matrices," *IEEE Transactions on Image Processing*, vol. 7, no. 11, pp. 1602-1609, Nov. 1998, doi: 10.1109/83.725367.

[38] A. Chu , C.M. Sehgal and J.F. Greenleaf , "Use of gray value distribution of run lengths for texture analysis",*Pattern Recognition Letters*, vol. 11, no. 6, pp. 415-419, Jun. 1990.

[39] Mary M. Galloway, "Texture analysis using gray level run lengths", *Computer Graphics and Image Processing* vol. 4, no. 2, pp. 172-179, Jun. 1975.

[40] B.R. Dasarathy and E.B. Holder ,"Image characterizations based on joint gray-level run-length distributions",*Pattern Recognition Letters* vol. 12, pp.497-502, Aug 1991.

[41] Xiaofei He, Deng Cai, Shuicheng Yan and Hong-Jiang Zhang, "Neighborhood preserving embedding," *Tenth IEEE International Conference on Computer Vision* (ICCV'05) Volume 1, Beijing, 2005, pp. 1208-1213 Vol. 2, doi: 10.1109/ICCV.2005.167.

[42] Gudigar, A., Chokkadi, S., Raghavendra, U., and Acharya, U. "An efficient traffic sign recognition based on graph embedding features." *Neural Computing and Applications.*vol. 31, pp. 1-13, Jul. 2019. https://doi.org/10.1007/s00521-017-3063-z

[43] Deng Cai, Xiaofei He, Kun Zhou, Jiawei Han, and Hujun Bao. "Locality sensitive discriminant analysis." *IJCAI'07: Proceedings of the 20th international joint conference on Artifical intelligence*, San Francisco, CA, USA, pp. 708-713, Dec 2007.

[44] O'Mahony, Michael "Sensory Evaluation of Food: Statistical Methods and Procedures." *CRC Press.*, 1986, pp. 487. ISBN 0-82477337-3

[45] V. Vapnik, "Statistical Learning Theory".*New York: Wiley*, 1998.

[46] Christopher J.C. Burges, "A Tutorial on Support Vector Machines for Pattern Recognition. " *Data Mining and Knowledge Discovery*,vol. 2, pp. 121–167, Jun. 1998. https://doi.org/10.1023/A:1009715923555

[47] N. Cristianini and J. Shame-Taylor, "Support Vector Machines and Other Kernel Based Learning Methods. Cambridge", *U.K.: Cambridge Univ. Press*, 2000.

[48] Svante Wold, Kim Esbensen, Paul Geladi, "Principal component analysis," *Chemometrics and Intelligent Laboratory Systems*,vol 2, no. 1–3, pp. 37-52, Aug. 1987

[49] Hyvärinen, A, and E Oja. "Independent component analysis: algorithms and applications." *Neural networks : the official journal of the International Neural Network Society* vol. 13, no. 4-5, pp. 411-30, Jun. 2000. doi:10.1016/s0893-6080(00)00026-5

[50] Alex Krizhevsky, Ilya Sutskever, and Geoffrey E. Hinton, "ImageNet Classification with Deep Convolutional Neural Networks." *Neural Information Processing Systems*, vol. 25, Jan. 2012.

[51] K. He, X. Zhang, S. Ren and J. Sun, "Deep Residual Learning for Image Recognition," *2016 IEEE Conference on Computer Vision and Pattern Recognition (CVPR)*, Las Vegas, NV, 2016, pp. 770-778, doi: 10.1109/CVPR.2016.90.

[52] Christian Szegedy, Wei Liu, Yangqing Jia, Pierre Sermanet *et al.*, "Going deeper with convolutions," *2015 IEEE Conference on Computer Vision and Pattern Recognition (CVPR)*, Boston, MA, 2015, pp. 1-9, doi: 10.1109/CVPR.2015.7298594.

[53] Elmekkawi SF, Mansour GM, Elsafty MSE, Hassanin AS, *et al.* "Prediction of Fetal Hypertrophic Cardiomyopathy in Diabetic Pregnancies Compared with Postnatal Outcome." *Clinical Medicine Insights: Women's Health* vol. 8, pp. 39-43, Dec. 2015.

**ANJAN GUDIGAR**, Ph.D., is currently working as a faculty in the Department of Instrumentation and Control Engineering, Manipal Institute of Technology, Manipal, India. He received his Ph.D. from Manipal Academy of Higher Education, India. His research interests include image processing, medical image analysis and pattern recognition. He has published several research papers in international conferences and journals. Please visit http://scholar.google.co.in/citations?user=qoe6EvsAAAAJ&hl=en for more details.

**DR. AKHILA VASUDEVA**, She received MBBS and MD in OBG from Kasturba medical college, Manipal Academy of Higher Education; DNB (OBG) from National Board of Examinations-India and MRCOG from London, UK. She is Professor and the chief consultant of Division of Fetal medicine at the department of Obstetrics and Gynecology, Kasturba medical college, Manipal Academy of Higher Education, Manipal, India. She has got teaching experience of 18 years. She is actively involved in the research and has published several research papers in the area of Obstetrics, gynecology and fetal medicine.

**JYOTHI SAMANTH** She received her Master of Science Degree in Echocardiography from Manipal academy of higher education, India. She is currently a faculty member with the department of cardiovascular technology, Manipal College of Health Professions, Manipal Academy of Higher Education, Manipal, India. She have several publications to her credits especially in the field of Echocardiography.

**DR. PADMAKUMAR R**, He received DM in cardiology from Sree Chitra Thirunal Institute for Medical Sceince, India. He is Professor and consultant interventional cardiologist in the department of cardiology, Kasturba medical college, Manipal Academy of Higher Education, Manipal, India. His focus on research include cardiac imaging, congenital heart disease, Coronary interventions etc. He has extensive teaching experience for > 20 years and published many research papers. He is keenly interested in research work.
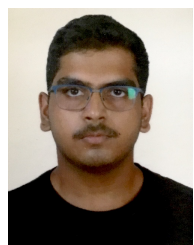
**U. RAGHAVENDRA** Ph.D., is working as faculty in the Department of Instrumentation and Control Engineering, Manipal Institute of Technology, Manipal, India. He received his Ph.D. from Manipal Academy of Higher Education, India. He has published several papers in refereed international SCI-IF journals and international conference proceedings. He has a patent to his credit and received an invention award from Intellectual Ventures, USA for his innovations in the year 2014. His major academic interests are in 3D Computer Vision, image processing and Medical image analysis. Please visit https://scholar.google.co.in/citations?user=3nzcDREAAAAJ&hl=en for more details.

**TAN RU SAN**, MBBS, is a senior Consultant, Department of Cardiology, National Heart Centre Singapore. His specialization is in non-invasive diagnostic cardiac imaging: cardiovascular magnetic resonance imaging, echocardiography and nuclear cardiology. His research interests include advanced cardiac imaging, cardiac biomechanics and computational modeling. He is also a site PI and member of the steering committees of multinational clinical trials of novel cardiology drugs, notably novel anticoagulants.

**CHINMAY DHARMIK** is perusing Bachelors in Instrumentation and Control Engineering from Manipal Institute of Technology, Manipal, India. He has been working in Digital Image processing, Medical Image Analysis and Computer Vision. And, visions a future in Embedded Systems and Image processing.

**EDWARD J CIACCIO**, PhD, is senior research scientist in the Department of Medicine, Division of Cardiology and the Celiac Disease Center, Columbia University, and honorary principal research fellow in the Department of Medicine, Division of Cardiology, Imperial College London. His work received a paper of the year award from Heart Rhythm journal in 2008, and he has been keynote speaker at the International Conference on Biomedical Engineering and Biotechnology (2013-2015) and Innovation in Medicine and Healthcare 2014. He was faculty speaker at the 1st Annual International Symposium on Ventricular Arrhythmias 2006, Atrial Signals 2015, the 13th Annual Congress of the European Cardiac Arrhythmia Society 2017, and Boston Signals Summit 2018. He has published over 100 peer-reviewed articles on such topics as biomedical signal processing of heart electrograms, and image processing of villous atrophy in celiac disease patients. In computational biology, Dr. Ciaccio has developed biophysical models of activation wavefront propagation for ventricular tachycardia and for atrial fibrillation. He is editor-in-chief of the journals Computers in Biology and Medicine, and Informatics in Medicine Unlocked.
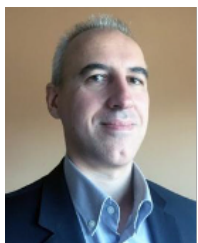
**FILIPPO MOLINARI** , PhD, DEng is Associate Professor in Biomedical Engineering on faculty of the Dept. of Electronics and Telecommunications of the Politecnico di Torino, Torino, Italy. His main research interests include medical imaging, ultrasound technologies, and noninvasive assessment of cerebral functions and autoregulation. Prof. Molinari is on the Editorial Board of several Journals in the field of bioengineering Complete profile available at:

https://scholar.google.it/citations?user=ttbUYiQAAAAJ&hl=it

**U. R. ACHARYA** , MTech, PhD, DEng, DSc is a senior faculty member at Ngee Ann Polytechnic, Singapore. He is also (i) Adjunct Professor at University of Malaya, Malaysia, (ii) Adjunct Professor at Asia University, Taiwan, (iii) Associate faculty at Singapore University of Social Sciences, Singapore and (iv) Adjunct Professor at University of Southern Queensland, Australia. He received his Ph.D. from National Institute of Technology Karnataka (Surathkal, India), DEng from Chiba University (Japan) and DSc from AGH University of Science and Technology, Poland. He has published more than 500 papers, in refereed international SCI-IF journals (345), international conference proceedings (42), books (17) with more than 34,500 citations in Google Scholar (with h-index of 98). He has worked on various funded projects, with grants worth more than 5 million SGD. He is ranked in the top 1% of the Highly Cited Researchers for the last five consecutive years (2016 to 2020) in Computer Science according to the Essential Science Indicators of Thomson. He is one among the World's Top 100,000 Scientists in 2019. He is on the editorial board of many journals and has served as Guest Editor for many journals.

● ● ●